Closely related rare-earth metal germanides RE 2Li 2Ge 3 and RE 3Li 4Ge 4 (RE = La-Nd, Sm): Synthesis, crystal chemistry, and magnetic properties

ARTICLE *in* INORGANIC CHEMISTRY · MARCH 2012

Impact Factor: 4.76 · DOI: 10.1021/ic202591j · Source: PubMed

3 AUTHORS, INCLUDING:

Sheng-Ping Guo
Yangzhou University
35 PUBLICATIONS **654** CITATIONS
SEE PROFILE

Svilen Bobev
University of Delaware
258 PUBLICATIONS **2,060** CITATIONS
SEE PROFILE

Inorganic Chemistry

Article

pubs.acs.org/IC

Closely Related Rare-Earth Metal Germanides $RE_2Li_2Ge_3$ and $RE_3Li_4Ge_4$ (RE = La−Nd, Sm): Synthesis, Crystal Chemistry, and Magnetic Properties

Sheng-Ping Guo, Tae-Soo You,† and Svilen Bobev*

Department of Chemistry and Biochemistry, University of Delaware, Newark, Delaware 19716, United States

Supporting Information

ABSTRACT: Reported are the syntheses, crystal structures, and magnetic susceptibilities of two series of closely related rare-earth metal−lithium germanides $RE_2Li_2Ge_3$ and $RE_3Li_4Ge_4$ (RE = La−Nd, Sm). All title compounds have been synthesized by reactions of the corresponding elements at high temperatures, and their structures have been established by single-crystal X-ray diffraction. $RE_2Li_2Ge_3$ phases crystallize in the orthorhombic space group *Cmcm* (No. 63) with the $Ce_2Li_2Ge_3$ structure type, while the $RE_3Li_4Ge_4$ phases crystallize in the orthorhombic space group *Immm* (No. 71) with the $Zr_3Cu_4Si_4$ structure type, respectively. Both of their structures can be recognized as the intergrowths of $MgAl_2Cu$- and AlB_2-like slabs, and these traits of the crystal chemistry are discussed. Temperature-dependent direct-current magnetization measurements indicate Curie−Weiss paramagnetism in the high-temperature regime for $RE_2Li_2Ge_3$ and $RE_3Li_4Ge_4$ (RE = Ce, Pr, Nd), while $Sm_2Li_2Ge_3$ and $Sm_3Li_4Ge_4$ exhibit Van Vleck-type paramagnetism. The data are consistent with the local-moment magnetism expected for RE^{3+} ground states. At temperatures below ca. 20 K, magnetic ordering transitions have been observed. The experimental results have been complemented by tight-binding linear muffin-tin orbital electronic-band-structure calculations.

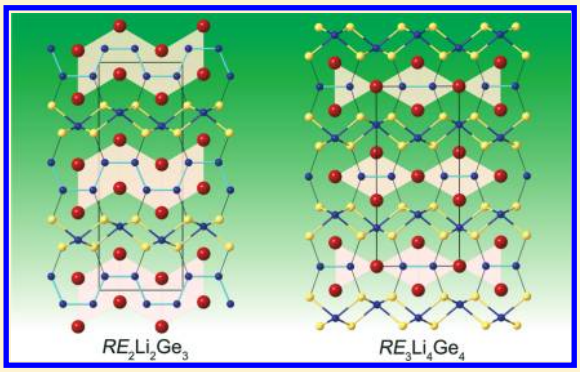

INTRODUCTION

The structures of many silicides, germanides, and stannides boast polyanionic clusters, chains, layers, and nets—all based on directional Tt−Tt interactions (Tt = tetrel).[1−4,6−11] Following years of continued research on tetrelides, especially germanides, our group has already reported several compounds whose structures feature two-dimensional (2D) layers, such as $CaGe_2$ (puckered $^2_\infty[Ge_2]$ layers),[2] RE_3Ge_5 (defect "honeycomb"-like layers),[3] and $RESn_{1\pm x}Ge_{1\pm x}$ ("square nets").[4,5] A wider variety of studied compounds appear to have "lower-dimensional" polyanions; for example, the structures of RE_2MgGe_2,[6] RE_2InGe_2,[7] $RE_{5-x}Mg_xGe_4$,[8] and $(Eu_{1-x}Ca_x)_4In_3Ge_4$[9] feature discrete Ge_2 dimers, whereas the structures of $RELiGe_2$,[10] and $(Sr_{1-x}Ca_x)_3In_2Ge_4$[11] are based on infinite $^1_\infty[Ge_2]$ chains with different topologies (zigzag or cis−trans). One could immediately recognize that the dimers and polymeric motifs are common for the compounds that contain Li or Mg−elements with relatively high Pauling electronegativity,[12] which may also contribute to the directional bonding. Indeed, prior investigations of the electronic structures of such polyanions have shown that the Tt−Tt interactions are intimately affected by the small and highly polarizable Li and Mg ions.[13]

Such ideas have already been explored by us in the recent study of $A_2(Li_{1-x}In_x)_2Ge_3$ (A = Sr, Ba, Eu).[14] Therein, we also noted the need for Li to be partially substituted by another element with more valence electrons, that is, In. The additional electrons were shown to be critical for the optimization of the Ge−Ge interactions.[14] This peculiarity in the electronic structure suggested that an "optimal" structure would exist if two more valence electrons per formula unit were available. Having carefully considered the roles of the alkaline-earth metals (and the nominally divalent Eu) in the overall chemical bonding, our attention was prompted in the direction of the early rare-earth metals; in $RE_2Li_2Ge_3$, they should exist as stable RE^{3+} ions and could provide the sought-after balance of valence electrons and atomic sizes.

With this paper, we present the synthesis, structural characterization, and magnetic susceptibilities of a total of 10 compounds belonging to two families $RE_2Li_2Ge_3$ and $RE_3Li_4Ge_4$ (RE = La−Nd, Sm). Their structures are closely related and may suggest the existence of a large homologous series. In addition to the structural relationships, we also discuss the results from the electronic structure calculations, which indicate an apparent "electron deficiency" in $RE_3Li_4Ge_4$. On the basis of analyses of the electronic and crystal structures, we argue that the $RE_2Li_2Ge_3$ phases are line compounds, whereas the $RE_3Li_4Ge_4$ phases are *not* devoid of crystallographic disorder and are best described as $RE_3Li_{4-x}Ge_{4+x}$ ($x \leq 0.1$).

Received: December 1, 2011
Published: February 14, 2012

   dx.doi.org/10.1021/ic202591j | *Inorg. Chem.* 2012, 51, 3119−3129

Table 1. Selected Crystal Data and Structure Refinement Parameters for the Compounds of the $RE_2Li_2Ge_3$ (RE = La−Nd, Sm) Series

empirical formula	$La_2Li_2Ge_3$	$Ce_2Li_2Ge_3$	$Pr_2Li_2Ge_3$	$Nd_2Li_2Ge_3$	$Sm_2Li_2Ge_3$
fw, g/mol	509.47	511.89	513.47	520.13	532.35
space group			*Cmcm* (No. 63)		
λ, Å			0.710 73		
T, K			200(2)		
a, Å	4.5311(19)	4.4724(4)	4.4432(10)	4.4222(7)	4.3720(5)
b, Å	19.001(8)	18.8254(16)	18.723(4)	18.658(3)	18.494(2)
c, Å	7.008(3)	6.9424(6)	6.9113(16)	6.8905(10)	6.8403(7)
V, Å^3	603.4(4)	584.51(9)	575.0(2)	568.54(10)	553.09(10)
Z	4	4	4	4	4
ρ_{calcd}, g/cm^3	5.608	5.817	5.932	6.077	6.393
μ(Mo Kα), cm^{-1}	284.69	303.46	319.63	334.50	368.44
GOF on F^2	1.006	1.081	1.057	1.113	1.071
R1 [$I > 2\sigma(I)$][a]	0.0351	0.0142	0.0265	0.0200	0.0191
wR2 [$I > 2\sigma(I)$][a]	0.0747	0.0333	0.0511	0.0472	0.0453
R_1 [all data][a]	0.0495	0.0171	0.0378	0.0219	0.0238
wR_2 [all data][a]	0.0823	0.0344	0.0554	0.0483	0.0484

[a] $R1 = \sum||F_o| - |F_c||/\sum|F_o|$; $wR2 = [\sum[w(F_o^2 - F_c^2)^2]/\sum[w(F_o^2)^2]]^{1/2}$, where $w = 1/[\sigma^2F_o^2 + (AP)^2 + BP]$ and $P = (F_o^2 + 2F_c^2)/3$; A and B are weight coefficients. For additional information, see the CIF in the Supporting Information.

EXPERIMENTAL SECTION

Synthesis. Handling of the starting materials [pure elements from Ames Lab, Alfa, or Aldrich (>99.9%)] was performed inside an argon-filled glovebox or under vacuum. All metals were used as received, except Li, whose surface had to be carefully cleaned with a blade every time the metal rod was cut. In a typical experiment, a mixture of elements with the desired stoichiometric ratio (total weight ca. 500 mg) was loaded into a Nb tube, which was then sealed by arc-welding under an Ar atmosphere. The welded Nb tube was subsequently enclosed in a fused silica tube, which was flame-sealed under vacuum (below discharge). To attain phase-pure $RE_2Li_2Ge_3$ (*RE* = La−Nd) samples, the tubes with the reactant mixtures inside were heated in tube furnaces to temperatures of 1253−1358 K (rate of 200 K/h) and equilibrated for 5 h, followed by a slow cooling to 1203 K at a rate of 5 K/h. The furnaces were then shut off and allowed to cool to room temperature. The best yield of $Sm_2Li_2Ge_3$ was obtained by subsequent annealing at 873 K for 3 days.

Phase-pure $RE_3Li_4Ge_4$ (*RE* = La, Ce) were obtained by a similar procedure, whereby the cooling step was extended to 573 K and the rate was changed to 10 K/h. Attempts to synthesize $RE_3Li_4Ge_4$ (*RE* = Pr, Nd) using the same heating profile failed, yielding instead complex mixtures of the targeted materials with the known *RE*LiGe phases[15] and some new ones (RE_4LiGe_4 and $RE_7Li_8Ge_{10}$), which will be discussed in a forthcoming article. To circumvent this synthetic problem, which could be attributed to the increased rare-earth metals' melting points,[16] arc-melted "RE_3Ge_4" precursors were reacted with 4 equiv of Li metal at 1253 K for 5 h, followed by cooling to 573 K at a rate of 10 K/h. $Sm_3Li_4Ge_4$ was never synthesized in 100% yield; the best sample was 80% pure (estimated from powder X-ray diffraction), with Sm_4LiGe_4 (Gd_5Si_4 type) being a common side product.

We note explicitly here that, besides the reaction schemes mentioned above, many other reactions were also tried in order to establish the best route to the synthesis of the title compounds. For example, a high-frequency induction furnace was employed to melt 2:2:3, 2:4:3, 3:8:4, and 3:4:4 mixtures of *RE*, Li, and Ge,[17] followed by annealing at 973 K for 3 days, adopted from the synthetic procedure published for the isostructural $RE_2Li_2Si_3$ compounds.[18] The results were still mixtures of at least two phases, although the target phases were the major products. The undertaken elaborate synthetic efforts suggest that both the $RE_2Li_2Ge_3$ and $RE_3Li_4Ge_4$ series span only the early to midearly rare-earth metals La, Ce, Pr, Nd, and Sm. Also, we found no evidence to suggest that the phase width of $RE_3Li_{4-x}Ge_{4+x}$ can be controlled via the loading stoichiometry; in all cases, $x \approx 0.1$ or smaller. Because of this very small phase width and for the sake of simplicity, the $RE_3Li_4Ge_4$ notation is used throughout the text.

Caution! *Some reactions mentioned above pose a risk because the reaction mixtures are heated to very high temperatures, where Nb and Ge could react, causing "leaks" of molten metals (and Li metal vapor) into the silica tubes. Therefore, the silica jackets in such reactions must be made sufficiently long, so that one of the ends is left protruding outside the furnace, and the reactions have to be monitored very carefully; in the event of a leak from the Nb ampules, a condensation at the end of the silica tube would indicate that heating should be stopped immediately.*

Crystallographic Studies. Powder X-ray diffraction patterns were taken at room temperature on a Rigaku MiniFlex powder diffractometer using Cu Kα radiation (θ−θ scan mode with a step size of 0.05° and a rate of 5 s/step). The instrument was enclosed and operated inside a nitrogen-filled glovebox, enabling us to handle air-sensitive materials. The collected powder X-ray diffraction patterns were primarily used for phase identification of the reaction products. Such analyses were carried out using the *JADE 6.5* software package. According to the powder X-ray diffraction data, all studied compounds, except $Sm_3Li_4Ge_4$, are pure phases. Powder X-ray diffraction patterns collected for specimens kept under an inert atmosphere and after several days of exposure to air were identical, suggesting that they are air-stable.

Single-crystal X-ray diffraction data were collected at 200 K using a Bruker SMART CCD-based diffractometer [three-circle goniometer; monochromated Mo Kα_1 radiation (λ = 0.710 73 Å)]. First, several crystals from each batch were selected and checked before the best ones were chosen for further analysis. Data collections were handled in four batch runs consisting of 456 frames each (frame width was 0.4° in ω and θ with a data acquisition rate of 8−12 s/frame). The angular range in 2θ was up to ca. 60°. Data collection was processed with Bruker's *SMART* software.[19a] Data reduction and integration, as well as global unit cell refinements, were done using *SAINT*.[19b] *SADABS* was used for semiempirical absorption correction based on equivalents.[20] The structure factors were sorted and merged by the subprogram *XPREP* in the *SHELXTL* software package,[21] which was also employed in the space-group determination. The structures were solved by direct methods and refined to convergence by full-matrix least-squares methods on F^2. Refined parameters included the scale factor, the atomic positions with anisotropic displacement parameters (except for Li), extinction coefficients, and occupancy factors. The refinements in all cases proceeded smoothly, and the final difference Fourier maps were flat with highest maxima and minima not larger than 1−1.5 e/Å^3. This, alongside the very good crystallographic parameters (Tables 1 and 2), is suggestive of the fact that all structures

dx.doi.org/10.1021/ic202591j | Inorg. Chem. 2012, 51, 3119−3129

Table 2. Selected Crystal Data and Structure Refinement Parameters for the $RE_3Li_4Ge_4$ (RE = La–Nd, Sm) Series[a]

empirical formula	$La_3Li_4Ge_4$	$Ce_3Li_4Ge_4$	$Pr_3Li_4Ge_4$	$Nd_3Li_4Ge_4$	$Sm_3Li_4Ge_4$
fw, g/mol	734.85	738.48	740.85	750.84	769.17
space group			*Immm* (No. 71)		
λ, Å			0.710 73		
T, K			200(2)		
a, Å	4.5122(15)	4.4625(5)	4.442(3)	4.4118(16)	4.3674(5)
b, Å	6.933(2)	6.8713(7)	6.844(4)	6.800(2)	6.7721(8)
c, Å	15.000(5)	14.823(2)	14.737(7)	14.649(5)	14.513(2)
V, Å^3	469.2(3)	454.52(8)	448.0(4)	439.5(3)	429.24(9)
Z	2	2	2	2	2
ρ_{calcd}, g/cm^3	5.201	5.396	5.492	5.674	5.951
μ(Mo Kα), cm^{-1}	258.85	276.46	291.21	307.76	338.87
GOF on F^2	1.081	1.056	1.080	1.013	1.117
R1 [$I > 2\sigma(I)$][b]	0.0221	0.0121	0.0176	0.0223	0.0213
wR2 [$I > 2\sigma(I)$][b]	0.0483	0.0294	0.0376	0.0526	0.0475
R1 [all data][b]	0.0241	0.0138	0.0188	0.0242	0.0240
wR2 [all data][b]	0.0491	0.0297	0.0380	0.0537	0.0485

[a]Because the $RE_3Li_4Ge_4$ formula is used throughout the text, this table does not refer to the refinements of $RE_3Li_{4-x}Ge_{4+x}$ [$x \leq 0.07(1)$]. The corresponding tables with the small Li and Ge disorder taken into consideration are provided as Supporting Information. [b]R1 = $\sum||F_o| - |F_c||/\sum|F_o|$; wR2 = $[\sum[w(F_o^2 - F_c^2)^2]/\sum[w(F_o^2)^2]]^{1/2}$, where $w = 1/[\sigma^2F_o^2 + (AP)^2 + BP]$ and $P = (F_o^2 + 2F_c^2)/3$; A and B are weight coefficients. For additional information, see the CIF in the Supporting Information.

Table 3. Atomic Coordinates and Equivalent Isotropic Displacement Parameters (U_{eq}[a]) for the Compounds of the $RE_2Li_2Ge_3$ (RE = La–Nd, Sm) Series

atom	site	x	y	z	U_{eq}/ Å^2
			$La_2Li_2Ge_3$		
La1	4*c*	0	0.4482(1)	$^1/_4$	0.010(1)
La2	4*c*	0	0.6598(1)	$^1/_4$	0.012(1)
Ge1	8*f*	0	0.0605(1)	0.0699(2)	0.011(1)
Ge2	4*c*	0	0.2801(1)	$^1/_4$	0.013(1)
Li	8*f*	0	0.1898(10)	0.560(3)	0.006(3)
			$Ce_2Li_2Ge_3$		
Ce1	4*c*	0	0.4483(1)	$^1/_4$	0.008(1)
Ce2	4*c*	0	0.6589(1)	$^1/_4$	0.009(1)
Ge1	8*f*	0	0.0610(1)	0.0689(2)	0.009(2)
Ge2	4*c*	0	0.2801(1)	$^1/_4$	0.011(1)
Li	8*f*	0	0.1900(4)	0.561(1)	0.007(1)
			$Pr_2Li_2Ge_3$		
Pr1	4*c*	0	0.4482(1)	$^1/_4$	0.008(1)
Pr2	4*c*	0	0.6587(1)	$^1/_4$	0.010(1)
Ge1	8*f*	0	0.0614(1)	0.0684(2)	0.009(1)
Ge2	4*c*	0	0.2801(1)	$^1/_4$	0.011(1)
Li	8*f*	0	0.1904(9)	0.562(2)	0.009(3)
			$Nd_2Li_2Ge_3$		
Nd1	4*c*	0	0.4481(1)	$^1/_4$	0.009(1)
Nd2	4*c*	0	0.6582(1)	$^1/_4$	0.010(1)
Ge1	8*f*	0	0.0615(1)	0.0679(1)	0.010(1)
Ge2	4*c*	0	0.2800(1)	$^1/_4$	0.011(1)
Li	8*f*	0	0.1904(5)	0.561(1)	0.012(2)
			$Sm_2Li_2Ge_3$		
Sm1	4*c*	0	0.4480(1)	$^1/_4$	0.011(1)
Sm2	4*c*	0	0.6577(1)	$^1/_4$	0.012(1)
Ge1	8*f*	0	0.0620(1)	0.0668(1)	0.012(1)
Ge2	4*c*	0	0.2798(1)	$^1/_4$	0.013(1)
Li	8*f*	0	0.1915(7)	0.564(2)	0.013(2)

[a]U_{ij} is defined as one-third of the trace of the orthogonalized U^{ij} tensor.

are devoid of disorder. However, in several cases, all within the $RE_3Li_4Ge_4$ series, we encountered a puzzling observation: the isotropic displacement parameters of the Li atoms were abnormally small and had to be constrained (Table 4). Subsequent refinements of the occupancy factors of the Li sites showed that they exceed unity by 10–25%. A possible explanation for these refinement problems involves the mixing of Li with a heavier element that can have similar coordination; such was the case with In and Li in $A_2(Li_{1-x}In_x)_2Ge_3$ (A = Sr, Ba, Eu).[22] Because all $RE_3Li_4Ge_4$ phases were obtained in high yields from stoichiometric reactions of the elements (and sometimes cocrystallization with $RE_2Li_2Ge_3$, whose structures were refined without such anomalies), the hypothesis for a "foreign" element here seemed unlikely. Therefore, our attention was focused on the supposition of a small admixture of Li and Ge (on the Li site) as a probable cause. Such conjecture is also corroborated by the apparent "electron shortage", analyzed at length in the Bonding and Electronic Structures section (vide infra).

While refinements of the structures of all compounds from the $RE_3Li_4Ge_4$ series did not make a compelling case for the existence of a Li–Ge positional disorder (viz. $RE_3Li_{4-x}Ge_{4+x}$), we found evidence for a small, but nonnegligible homogeneity range in the isostructural stannide $Ce_3Li_{4-x}Sn_{4+x}$ (Supporting Information). According to the structure refinements for the latter, the Li occupancy factor, when freed, exceeded unity by more than 100%. This fact clearly confirms the origin of the disorder and its dependence on the Z number of the substituting element. Refining Li and Sn on the same site led to a statistical 0.925:0.075(5) mixture, evidently, more difficult to be accounted for in the cases of Li and Ge. These experimental facts are reconciled with analyses of the electronic structure and some geometric considerations, discussed later on.

In the last refinement cycles, the atomic positions were standardized by employing *STRUCTURE TIDY*.[23] Important crystallographic data, atomic positions, selected interatomic distances, and atomic displacement parameters of the series are listed in Tables 1–6. CIFs have also been deposited with Fachinformationszentrum Karlsruhe, 76344 Eggenstein-Leopoldshafen, Germany [fax (49) 7247-808-666; e-mail crysdata@fiz.karlsruhe.de] with depository numbers CSD-423834 for $La_2Li_2Ge_3$, CSD-423835 for $Ce_2Li_2Ge_3$, CSD-423836 for $Pr_2Li_2Ge_3$, CSD-423837 for $Nd_2Li_2Ge_3$, CSD-423838 for $Sm_2Li_2Ge_3$, CSD-423839 for $La_3Li_4Ge_4$, CSD-423840 for $Ce_3Li_4Ge_4$, CSD-423841 for $Pr_3Li_4Ge_4$, CSD-423853 for $Nd_3Li_4Ge_4$, and CSD-423842 for $Sm_3Li_4Ge_4$.

Magnetic Susceptibility Measurements. Field-cooled (FC) direct-current (dc) magnetization measurements were performed in a Quantum Design PPMS from 5 to 300 K in an applied magnetic field of 5000 Oe. To ensure reproducibility, specimens from at least two different reaction batches were measured. In all cases, the samples (ca. 100 mg of a freshly prepared polycrystalline material) were

dx.doi.org/10.1021/ic202591j | *Inorg. Chem.* 2012, 51, 3119–3129

Table 4. Atomic Coordinates and Equivalent Isotropic Displacement Parameters (U_{eq}[a]) for the Compounds of the $RE_3Li_4Ge_4$ (RE = La−Nd, Sm) Series

atom	site	x	y	z	U_{eq}/ Å^2
			$La_3Li_4Ge_4$		
La1	2a	0	0	0	0.010(1)
La2	4j	1/2	0	0.3673(1)	0.010(1)
Ge1	4h	0	0.1820(1)	1/2	0.010(1)
Ge2	4i	0	0	0.2129(1)	0.012(1)
Li	8l	0	0.311(2)	0.3304(7)	0.012(2)
			$Ce_3Li_4Ge_4$		
Ce1	2a	0	0	0	0.010(1)
Ce2	4j	1/2	0	0.3680(1)	0.010(1)
Ge1	4h	0	0.1835(1)	1/2	0.010(1)
Ge2	4i	0	0	0.2132(1)	0.011(1)
Li	8l	0	0.3109(8)	0.3298(4)	0.004(1)
			$Pr_3Li_4Ge_4$		
Pr1	2a	0	0	0	0.008(1)
Pr2	4j	1/2	0	0.3685(1)	0.009(1)
Ge1	4h	0	0.1841(1)	1/2	0.009(1)
Ge2	4i	0	0	0.2134(1)	0.010(1)
Li	8l	0	0.3094(9)	0.3293(4)	0.003(1)
			$Nd_3Li_4Ge_4$		
Nd1	2a	0	0	0	0.008(1)
Nd2	4j	1/2	0	0.3689(1)	0.009(1)
Ge1	4h	0	0.1848(1)	1/2	0.009(1)
Ge2	4i	0	0	0.2134(1)	0.010(1)
Li	8l	0	0.307(2)	0.3285(7)	0.005(2)
			$Sm_3Li_4Ge_4$		
Sm1	2a	0	0	0	0.010(1)
Sm2	4j	1/2	0	0.3698(1)	0.011(1)
Ge1	4h	0	0.1860(2)	1/2	0.011(1)
Ge2	4i	0	0	0.2137(1)	0.011(1)
Li	8l	0	0.310(2)	0.3293(8)	0.008[b]

[a] U_{ij} is defined as one-third of the trace of the orthogonalized U^{ij} tensor. [b] Constrained.

secured in gel capsules, using cotton. The raw magnetization data were collected for the holder contribution and converted to molar susceptibility ($\chi_m = M/H$). Zero-field-cooled (ZFC) measurements were carried out from 5 to 35 K under a field of 5000 Oe. Field sweeps (up to 70 kOe) for $Ce_2Li_2Ge_3$ were done at 2 K.

Computational Details. Tight-binding linear muffin-tin orbital (TB-LMTO) calculations were carried out using the *LMTO47* program.[24] This package employs the atomic sphere approximation (ASA) method, in which space is filled with overlapping Wigner−Seitz (WS) atomic spheres.[25] The symmetry of the potential is considered spherical inside each WS sphere, and a combined correction is used to take into account the overlapping part.[26] The radii of the WS spheres were obtained by requiring that the overlapping potential be the best possible approximation to the full potential and were determined by an automatic procedure. Exchange and correlation were treated by the local density approximation.[27] All relativistic effects, except spin−orbit coupling, were taken into account using a scalar relativistic approximation.[28] The WS radii are as follows: La = 1.94−1.97 Å, Li = 1.43 Å, and Ge = 1.45−1.64 Å for $La_2Li_2Ge_3$ and La = 2.05−2.10 Å, Li = 1.45 Å, and Ge = 1.49−1.72 Å for $La_3Li_4Ge_4$. The *k*-space integrations were conducted by the tetrahedron method, and the self-consistent charge density was obtained using 16 × 16 × 8 *k* points for $La_2Li_2Ge_3$ and 16 × 16 × 16 for $La_3Li_4Ge_4$ in the Brillouin zone. The La 6p, Ge 4d, and Li 2p orbitals were treated by the Löwdin downfolding technique.[29]

RESULTS AND DISCUSSION

Structures. The $RE_2Li_2Ge_3$ (*RE* = La−Nd, Sm) compounds crystallize in the orthorhombic space group *Cmcm* ($Ce_2Li_2Ge_3$ structure type, Pearson code *oC*28).[30] The archetype $Ce_2Li_2Ge_3$ had been identified by Pavlyuk et al. from powder X-ray diffraction data,[31] and here for the first time, we provide the atomic coordinates and the displacement parameters refined from single-crystal work. Other structurally characterized compounds with the same structure include the silicide $Nd_2Li_2Si_3$,[18] the germanides $Sr_2Li_{0.94}Mg_{1.06}Ge_3$,[32] $Eu_2Li_{1.16}Mg_{0.84}Ge_3$,[32] $Eu_2Li_{1.36}In_{0.64}Ge_3$,[14] and $Sr_2Li_{1.45}In_{0.55}Ge_3$,[14] and the stannides $Eu_2Li_{0.9}Mg_{1.1}Sn_3$,[33] $Sr_2Li_{0.74}Mg_{1.26}Sn_3$,[33] and $Sr_2LiMgSn_3$.[34] $RE_2Li_2Si_3$ (*RE* = La−Pr, Sm) have also been reported, although they have only been recognized from their powder X-ray diffraction patterns.[18] Notice that, except for $Ce_2Li_2Ge_3$ and $Nd_2Li_2Si_3$, all other compounds are known to exhibit Li/Mg or Li/In disorder, an issue that is discussed in several earlier publications[14,33] and is related to the electronic structure (vide infra).

Figure 1 shows a representation of the structure; relevant crystallographic parameters are tabulated in Tables 1, 3, and 5.

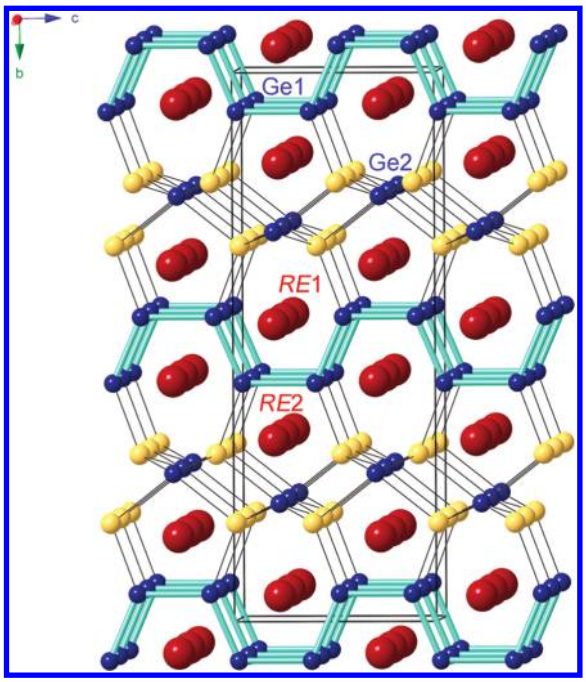

Figure 1. Ball-and-stick representation of the orthorhombic structure of $RE_2Li_2Ge_3$ (RE = La−Nd, Sm). The projection is approximately along the *a* axis, and the unit cell is outlined. The RE atoms are shown as deep-red spheres, and the Ge atoms are drawn as blue spheres. The $^1_\infty[Ge_2]$ chains are emphasized. The Li atoms (in yellow) are shown as connected to four neighboring Ge atoms, forming slabs of fused $LiGe_4$ tetrahedra.

Because the $Ce_2Li_2Ge_3$-type structure has been discussed previously, here we will only provide a brief description. The asymmetric unit of the structure contains five crystallographically unique sites: two for the rare-earth metal atoms, one for the Li atom, and two for the Ge atoms. The multiplicity and site symmetry for the two Ge atomic positions are different; hence, it is not surprising that they have different "chemical roles": Ge1 atoms form infinite $^1_\infty[Ge_2]$ chains of alternating trans and cis bonds, running in a direction parallel to the *c* axis, while Ge2 atoms are isolated. The two types of Ge1−Ge1 bonds are subtly different in terms of their lengths: the trans bonds [2.470(2)−2.500(3) Å] are

dx.doi.org/10.1021/ic202591j | Inorg. Chem. 2012, 51, 3119−3129

Table 5. Important Interatomic Distances (Å) for the Compounds of the $RE_2Li_2Ge_3$ (RE = La–Nd, Sm) Series

$La_2Li_2Ge_3$		$Ce_2Li_2Ge_3$		$Pr_2Li_2Ge_3$	
La1–Ge1	3.1918(13) × 4	Ce1–Ge1	3.1516(4) × 4	Pr1–Ge1	3.1320(9) × 4
La1–Ge2	3.193(3)	Ce1–Ge2	3.1652(8)	Pr1–Ge2	3.1470(19)
La1–Ge1	3.3586(14) × 4	Ce1–Ge1	3.3388(4) × 4	Pr1–Ge1	3.3164(10) × 4
La2–Ge1	3.2073(14) × 4	Ce2–Ge1	3.1589(4) × 4	Pr2–Ge1	3.1356(9) × 4
La2–Ge2	3.2186(18) × 2	Ce2–Ge2	3.1958(6) × 2	Pr2–Ge2	3.1791(13) × 2
La2–Li	3.190(13) × 4	Ce2–Li	3.165(5) × 4	Pr2–Li	3.152(11) × 4
La2–Li	3.152(19) × 2	Ce2–Li	3.132(7) × 2	Pr2–Li	3.110(16) × 2
Ge1–Ge1	2.500(3)	Ge1–Ge1	2.4865(9)	Ge1–Ge1	2.484(2)
Ge1–Ge1	2.524(3)	Ge1–Ge1	2.5145(10)	Ge1–Ge1	2.510(2)
Li–Ge1	2.620(19)	Li–Ge1	2.592(7)	Li–Ge1	2.579(16)
Li–Ge2	2.690(10) × 2	Li–Ge2	2.652(4) × 2	Li–Ge2	2.633(8) × 2
Li–Ge2	2.768(19)	Li–Ge2	2.748(7)	Li–Ge2	2.732(16)
$Nd_2Li_2Ge_3$			$Sm_2Li_2Ge_3$		
Nd1–Ge1	3.1175(5) × 4		Sm1–Ge1	3.0837(6) × 4	
Nd1–Ge2	3.1366(10)		Sm1–Ge2	3.1102(13)	
Nd1–Ge1	3.3073(6) × 4		Sm1–Ge1	3.2862(7) × 4	
Nd2–Ge1	3.1176(5) × 4		Sm2–Ge1	3.0785(7) × 4	
Nd2–Ge2	3.1710(7) × 2		Sm2–Ge2	3.1432(9) × 2	
Nd2–Li	3.134(7) × 4		Sm2–Li	3.128(9) × 4	
Nd2–Li	3.112(9) × 2		Sm2–Li	3.1432(9) × 2	
Ge1–Ge1	2.4790(11)		Ge1–Ge1	2.4695(16)	
Ge1–Ge1	2.5099(12)		Ge1–Ge1	2.5058(16)	
Li–Ge1	2.561(9)		Li–Ge1	2.556(13)	
Li–Ge2	2.627(5) × 2		Li–Ge2	2.584(6) × 2	
Li–Ge2	2.716(9)		Li–Ge2	2.698(12)	

systematically shorter than the cis bonds [2.506(2)–2.524(3) Å], respectively.

The narrow variation of the refined Ge–Ge distances shows a correlation with the gradual decrease of the atomic sizes on going from La to Sm,[12] and the corresponding monotonic decrease in the unit cell parameters (Table 1). However, we must recognize that the shortest Ge–Ge bonds are reported for two compounds that have the largest unit cell volumes: $Eu_2Li_{1.36}In_{0.64}Ge_3$ [d_{Ge-Ge} = 2.475 (1) and 2.502(1) Å] and $Eu_2Li_{1.11}Mg_{0.89}Ge_3$ [d_{Ge-Ge} = 2.472 (1) and 2.506(1) Å].[14] Clearly, the characteristics of the Ge–Ge bonding here indicate that the structure responds to the variable valence electron count; hence, some degree of depopulation of the Ge π^* orbitals must be considered. These traits of the bonding have also been mentioned in other publications on related structures,[13,14,32–34] including other examples with zigzag Ge chains, such as *RE*LiGe$_2$ (*RE* = La–Sm, Eu).[10]

Each Li atom in the structure is tetrahedrally surrounded by one Ge1 and three Ge2 atoms. The average Li–Ge distances are on the order 2.55–2.75 Å, with Li–Ge1 being the shorter ones (Table 5). These values are close to the sum of Pauling's radii of Li (1.225 Å) and Ge (1.242 Å),[12] indicating that the Li–Ge interactions have considerable covalent character. As a consequence of that, the structure description can be given emphasizing the polyanionic $^3_\infty[Li_2Ge_3]$ network instead of the $^1_\infty[Ge_2]$ chains. The Li–Ge distances are comparable to those in *RE*LiGe$_2$ (*RE* = La–Nd, Sm),[10] but the ones observed in $A_2(Li_{1-x}In_x)Ge_3$ (*A* = Sr, Eu)[14] and $RE_3Li_4Ge_4$ (*RE* = La–Nd, Sm) are slightly longer, which can be attributed to the mixing of In and Li and of Ge and Li, respectively.

The $RE_3Li_4Ge_4$ (*RE* = La–Nd, Sm) compounds crystallize in the orthorhombic space group *Immm* ($Zr_3Cu_4Si_4$ structure type, Pearson code *oI*22).[30] Until now, more than 60 compounds have been reported with this atomic arrangement, and the majority of them contain late transition metals, Cu or Ag in particular.[30] $Sr_3Li_4Sb_4$[35] and $Ba_3Li_4As_4$[36] are also known to form with this

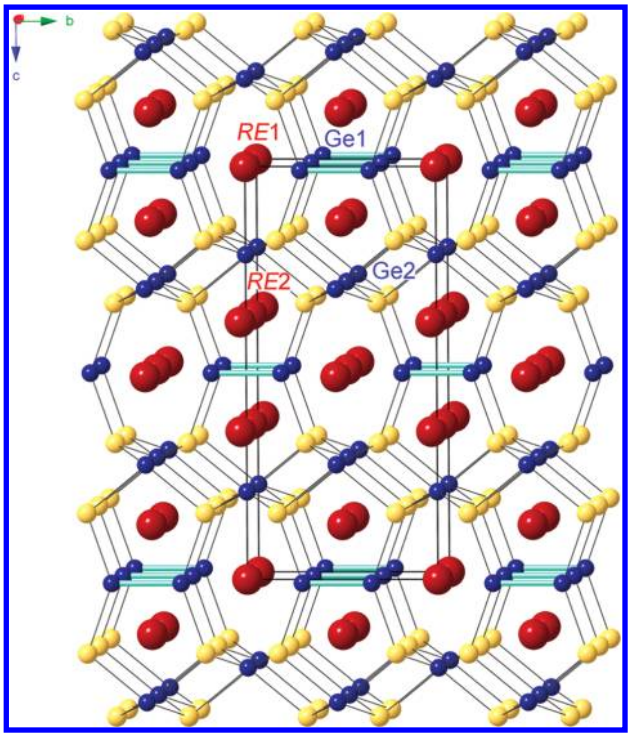

Figure 2. Ball-and-stick representation of the orthorhombic structure of $RE_3Li_4Ge_4$ (RE = La–Nd, Sm). The projection is approximately along the *a* axis, and the unit cell is outlined. The RE atoms are shown as deep-red spheres, and the Ge atoms are drawn as blue spheres. The [Ge_2] dumbbells are emphasized. The Li atoms (in yellow) are shown as connected to four neighboring Ge atoms, forming slabs of fused $LiGe_4$ tetrahedra.

dx.doi.org/10.1021/ic202591j | Inorg. Chem. 2012, 51, 3119–3129

Table 6. Important Interatomic Distances (Å) for the Compounds of the $RE_3Li_4Ge_4$ (RE = La–Nd, Sm) Series

$La_3Li_4Ge_4$		$Ce_3Li_4Ge_4$		$Pr_3Li_4Ge_4$	
La1–Ge1	3.1542(10) × 4	Ce1–Ge1	3.1159(5) × 4	Pr1–Ge1	3.0994 (13) × 4
La1–Ge2	3.1939(14) × 2	Ce1–Ge2	3.1609(6) × 2	Pr1–Ge2	3.1445(17) × 2
La2–Ge1	3.2623(8) × 4	Ce2–Ge1	3.2242(4) × 4	Pr2–Ge1	3.2059(12) × 4
La2–Ge2	3.2333(10) × 2	Ce2–Ge2	3.2002(5) × 2	Pr2–Ge2	3.1870(13) × 2
La1–Li	3.645(8) × 6	Ce1–Li	3.610(4) × 6	Pr1–Li	3.600(5) × 6
La2–Li	3.168(7) × 4	Ce2–Li	3.140(4) × 4	Pr2–Li	3.122(5) × 4
La2–Li	3.243(11) × 2	Ce2–Li	3.207(6) × 2	Pr2–Li	3.193(7) × 2
Ge1–Ge1	2.524(2)	Ge1–Ge1	2.5213(11)	Ge1–Ge1	2.5199(18)
Li–Ge1	2.696(11)	Li–Ge1	2.671(6)	Li–Ge1	2.658(7)
Li–Ge2	2.690(6) × 2	Li–Ge2	2.660(3) × 2	Li–Ge2	2.651(4) × 2
Li–Ge2	2.783(10)	Li–Ge2	2.747(6)	Li–Ge2	2.721(6)
$Nd_3Li_4Ge_4$			$Sm_3Li_4Ge_4$		
Nd1–Ge1	3.0756(10) × 4		Sm1–Ge1	3.0480(8) × 4	
Nd1–Ge2	3.1268(14) × 2		Sm1–Ge2	3.1008(11) × 2	
Nd2–Ge1	3.1834(9) × 4		Sm2–Ge1	3.1505(6) × 2	
Nd2–Ge2	3.1706(11) × 2		Sm2–Ge2	3.1471(9) × 2	
Nd1–Li	3.591(8) × 6		Sm1–Li	3.544(9) × 6	
Nd2–Li	3.095(8) × 4		Sm2–Li	3.087(8) × 4	
Nd2–Li	3.175(10) × 2		Sm2–Li	3.162(11) × 2	
Ge1–Ge1	2.514(2)		Ge1–Ge1	2.519(2)	
Li–Ge1	2.646(10)		Li–Ge1	2.617(11)	
Li–Ge2	2.639(6) × 2		Li–Ge2	2.609(6) × 2	
Li–Ge2	2.684(10)		Li–Ge2	2.698(12)	

structure, but the title compounds are the first germanides containing lithium that belong to this family.

The structure is schematically represented in Figure 2. There are five crystallographically unique sites in the asymmetric unit: two for the rare-earth metal atoms, one for the Li atom, and two for the Ge atoms. Ge1 atoms form Ge_2 dimers, aligned in the direction of the *b* axis, while Ge2 atoms are isolated. The Ge1–Ge1 distances in the series fall in the narrow interval 2.514(2)–2.524(2) Å (Table 6) and vary negligibly with the monotonic decrease in the unit cell volumes upon moving from La to Sm (Table 2). The refined Ge–Ge bond lengths compare well with the values reported for some other structures containing rare-earth metals and Ge_2 dimers, such as RE_2InGe_2 [d_{Ge-Ge} = 2.504(5)–2.512(2) Å][7] and RE_2MgGe_2 [d_{Ge-Ge} = 2.506(2)–2.548(1) Å].[6] Some other examples with simple covalent Ge–Ge interactions include, but are not limited to, $CaGe_2$ [d_{Ge-Ge} = 2.541(1) Å][2] and Ca_5Ge_3 [d_{Ge-Ge} = 2.575(1) Å].[1a]

The rare-earth metal atoms form trigonal prisms, which are centered by Ge atoms. The closest *RE*–*RE* contacts are on the order of 3.9–4.0 Å, much longer than the corresponding RE–*RE* contacts in the elemental crystal structures.[30] Each rare-earth metal atom at the *RE*1 site is at the center of a slightly distorted octahedron of Ge atoms; each rare-earth metal atom at the *RE*2 site is at the center of a coordination polyhedron that can be described as a trigonal prism formed by six Ge atoms.

Structural Relationships. Despite the differences in the bonding characteristics, as described above, both the $RE_2Li_2Ge_3$ and $RE_3Li_4Ge_4$ (*RE* = La–Nd, Sm) structures are closely related. Recognizing that each crystal structure can be "cut" into slabs resembling the known AlB_2 and $MgAl_2Cu$ (aka Re_3B) structure types[30] helps to illustrate this schematic (not rigorous crystallographic) interpretation of their extended symmetry. The analogy is depicted in Figure 3: the two slabs with composition "$REGe_2$" (AlB_2-like motif) and "$RELi_2Ge$" ($MgAl_2Cu$-like motif) can be easily discerned from the coloring scheme. Extending the idea even further allows the $RE_2Li_2Ge_3$ structure (represented as $RE_4Li_4Ge_6$) to be described as an intergrowth of $REGe_2$ (AlB_2 structure type) and $RE_3Li_4Ge_4$ ($Zr_3Cu_4Si_4$ structure type) fragments in an equimolar fashion, as shown in Figure 4. Here, it must be pointed out that, in some older works,[37] the $Zr_3Cu_4Si_4$ structure has been erroneously related to the AlB_2 and $ThCr_2Si_2$ (ternary version of $BaAl_4$) type structures. Although there are some similarities in the bonding patterns between the $ThCr_2Si_2$ and $MgAl_2Cu$ structures (as shown in Figure S2 in the Supporting Information), using these "building blocks" cannot produce the correct stoichiometry of the $RE_2Li_2Ge_3$ compounds; notice that the formula units "$RELi_2Ge$" ($MgAl_2Cu$ structure type) and "$RELi_2Ge_2$" ($ThCr_2Si_2$ structure type) differ by one Ge atom.

On the basis of the identified structural associations, the structure of the $RE_2Li_2Ge_3$ compounds can then be thought to be an intergrowth of the imaginary $REGe_2$ and $RELi_2Ge$ phases in a 1:1 ratio, while the structure of the $RE_3Li_4Ge_4$ compounds can be considered to be their 1:2 intergrowth.[38] One can extend this idea further and can propose other possible combinations of such fragments, assuming that a homologous series $[REGe_2]_n[RELi_2Ge]_m$ exists. $RE_2Li_2Ge_3$ will be the simplest member, described with n = 1 and m = 1. The next homologue is realized when n = 1 and m = 2; this is the case of $RE_3Li_4Ge_4$. Higher homologues are yet to be synthesized and characterized; preliminary results indicate the existence of $Ce_7Li_8Ge_{10}$, which is the member with n = 3 and m = 4.[39]

Bonding and Electronic Structures. Computations based on density functional theory were carried out for $La_2Li_2Ge_3$ and $La_3Li_4Ge_4$ as representatives of each structure. The total and partial density of states (DOS) curves for $La_2Li_2Ge_3$ and $La_3Li_4Ge_4$ and the crystal orbital Hamilton populations (COHPs) calculated for the Ge–Ge and Li–Ge bonds in $La_2Li_2Ge_3$ and $La_3Li_4Ge_4$ are plotted in Figures 5 and 6, respectively.

As can be seen from Figure 5, there is a deep pseudogap at the Fermi level (E_F) for $La_2Li_2Ge_3$. This local energy minimum corresponds to 20 valence electrons per formula and is in agreement with the earlier conclusions regarding the isostructural, but not isoelectronic, $A_2(Li_{1-x}In_x)_2Ge_3$ (*A* = Sr, Eu) phases.[14] A significant mixing between Li and Ge states with

dx.doi.org/10.1021/ic202591j | Inorg. Chem. 2012, 51, 3119–3129

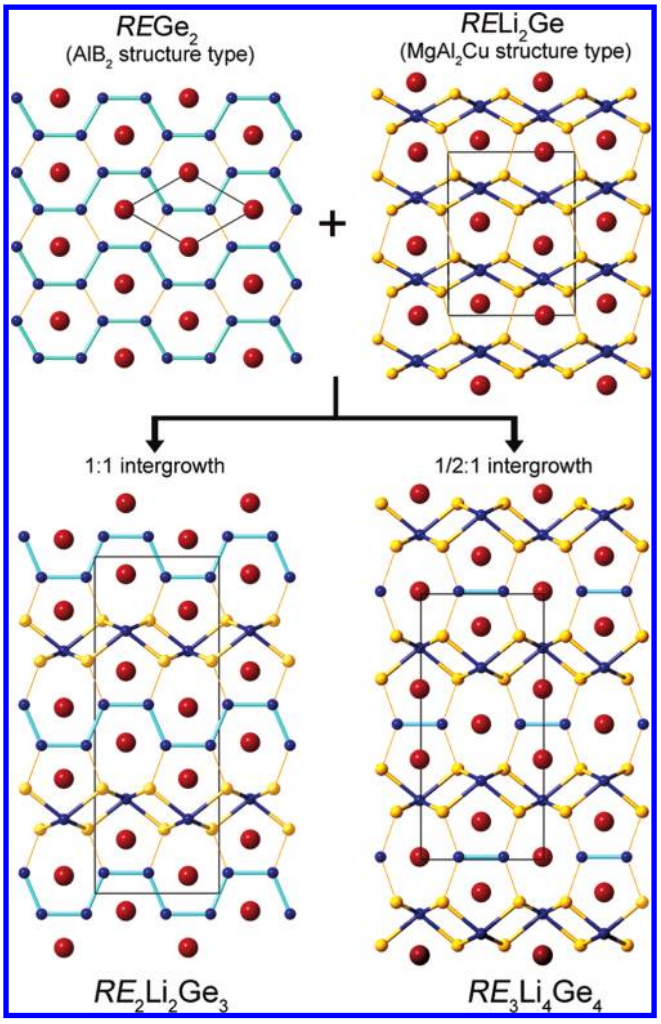

Figure 3. Schematic representation of the structural relationship between $RE_2Li_2Ge_3$ and $RE_3Li_4Ge_4$ (RE = La–Nd, Sm) and the hypothetical $REGe_2$ (AlB_2 structure type) and $RELi_2Ge$ ($MgAl_2Cu$ structure type) compounds. The $RE_2Li_2Ge_3$ and $RE_3Li_4Ge_4$ structures can be considered as 1:1 and 1:2 intergrowths of these common bonding arrangements, suggesting that higher homologues might also exist. See the text for details.

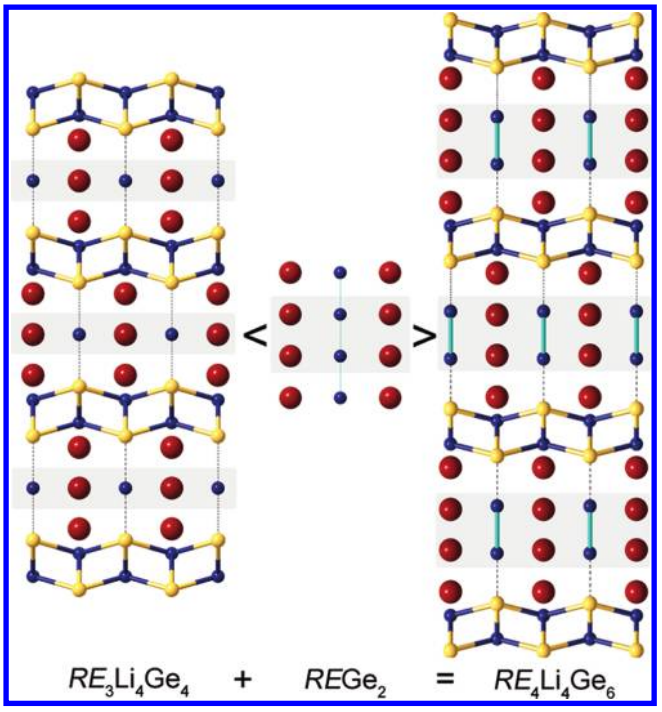

Figure 4. Schematic representation of how the $RE_2Li_2Ge_3$ structure (rewritten for convenience as $RE_4Li_4Ge_6$) can be derived from the structure of $RE_3Li_4Ge_4$, via "intercalation" of $REGe_2$ slabs (AlB_2-like). See the text for details.

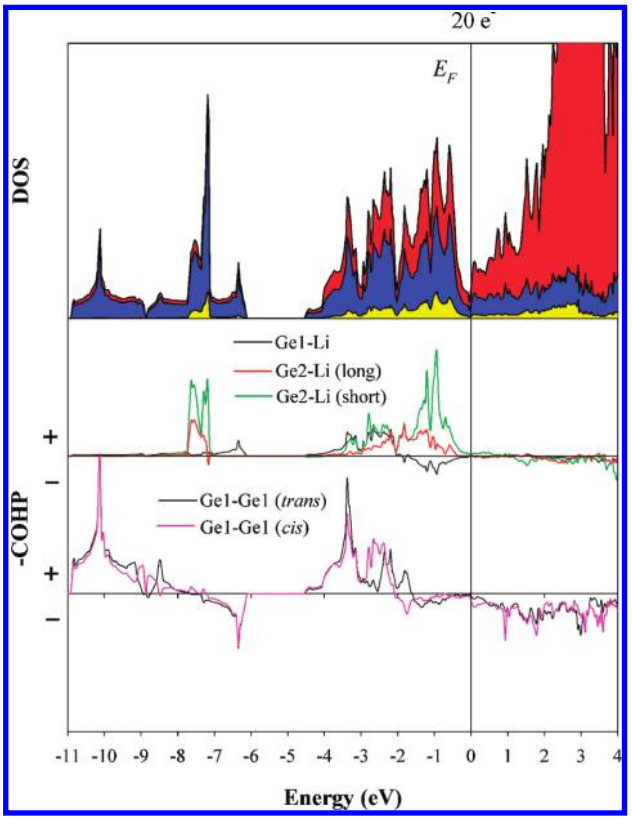

Figure 5. Calculated DOS and COHP for $La_2Li_2Ge_3$. The total and partial DOSs (Ge PDOS, blue area; Li PDOS, yellow area) are plotted. The Fermi level is chosen as the energy reference at 0 eV.

some participation of La orbitals is observed between −4.5 eV and E_F, which indicates that all atoms participate in covalent-type interactions and that neither La nor Li should be regarded as simple electron donors. According to their COHP, both the cis and trans Ge1–Ge1 interactions are nonbonding to weakly antibonding at the Fermi level; the two types of Ge–Ge bonds show increased antibonding character beyond the Fermi level (Figure 5). Just like in the $A_2(Li_{1-x}In_x)_2Ge_3$ case,[14] the trans bonds are slightly stronger (shorter) than the cis bonds, and this can be attributed to the decrease of their antibonding character.

On the basis of the computed electronic structure of $La_2Li_2Ge_3$, one can expect that the valence rules can be applied and the electron count can be rationalized by following the Zintl–Klemm formalism.[40] Recall that the structure has two Ge atoms, one isolated and one forming the $^1_\infty[Ge_2]$ cis/trans-chains; the formal charge of each isolated Ge atom should be "4–", and each two-bonded Ge atom should carry a formal charge of "2–". Assigning the rare-earth metal and the Li atoms as electron donors, although it is an oversimplification, yields the charge-balanced formula $(La^{3+})_2(Li^+)_2(Ge^{4-})(Ge^{2-})_2$. This description, of course, does not take into account the fact that La and Li cannot provide the full eight electrons for Ge bonding. Hence, the incomplete charge transfer will require the $^1_\infty[Ge_2]$ cis/trans

dx.doi.org/10.1021/ic202591j | Inorg. Chem. 2012, 51, 3119–3129

chains to be treated as polyacetylene-like chains of alternating single and double bonds. The relatively short Ge−Ge bonds (along with the already discussed differences between the cis and trans bonds) support this conclusion.

As discussed earlier, there is crystallographic evidence for a small admixture of Ge at the Li site in the compounds of the $RE_3Li_4Ge_4$ series. However, because the disorder is very small, it is practically impossible to establish a model structure for accurate calculations; therefore, $La_3Li_4Ge_4$, without any Li and Ge mixing was used instead. Figure 6 displays the total DOS

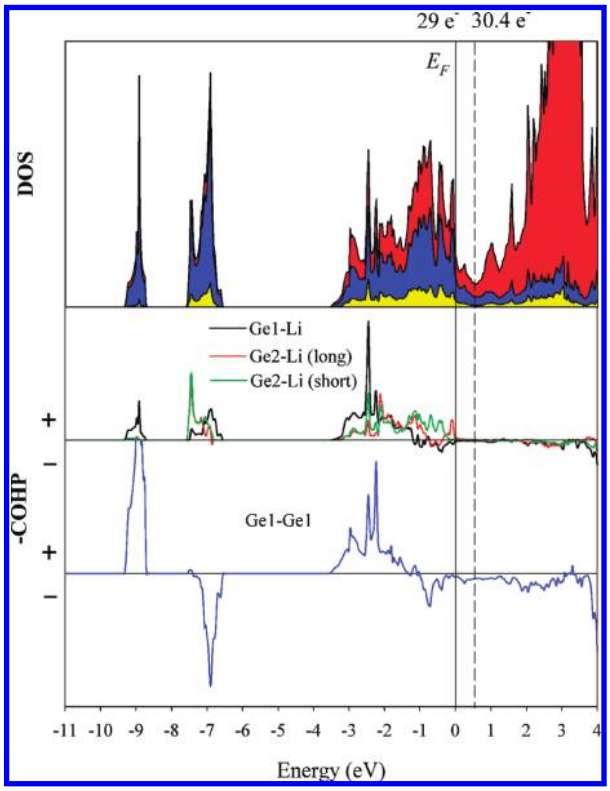

Figure 6. Calculated DOS and COHP for $La_3Li_4Ge_4$. The Fermi level is chosen as the energy reference at 0 eV. The total and partial DOSs (Ge PDOS, blue area; Li PDOS, yellow area) are plotted. The dashed line indicates the Fermi level for a rigid band system with 30.4 valence electrons, corresponding to the deep local minimum.

calculated for $La_3Li_4Ge_4$, with the components from each La, Li, and Ge atom. As seen from the plot, the Fermi level corresponding to 29 valence electrons is in an area of relatively high DOS, ca. 0.51 eV below a local DOS minimum. Such characteristics of the total DOS indicate that the stoichiometric compound $La_3Li_4Ge_4$ is electronically unfavorable, and a slightly higher valence electron concentration (VEC) is required in order for the structure to achieve greater stability. This argument supports the observed partial substitution of Li with the electron-richer Ge (vide supra), which seems to be the way nature has chosen to increase the number of valence electrons to optimal levels. A similar "mechanism" for augmenting the electron count has also been seen for a number of related phases,[22] such as $Eu_2Li_{1.36}In_{0.64}Ge_3$,[14] $Sr_2Li_{1.45}In_{0.55}Ge_3$,[14] $Sr_2Li_{0.94}Mg_{1.06}Ge_3$,[32] $Eu_2Li_{1.16}Mg_{0.84}Ge_3$,[32] $Eu_2Li_{0.9}Mg_{1.1}Sn_3$,[33] and $Sr_2Li_{0.74}Mg_{1.26}Sn_3$.[33]

Arguably, the refinements of the Li−Ge ratios for the $RE_3Li_{4-x}Ge_{4+x}$ series are not convincing enough because of the magnitude of the effect and the relatively large uncertainties (viz., $Sm_3Li_{3.93}Ge_{4.07(1)}$; VEC = 29.2 electrons/formula; see the Supporting Information). However, refinements for the stannide analogue $Ce_3Li_{3.69}Sn_{4.31(1)}$ with VEC = 29.9 electrons/formula clearly show that, through replacement of some of the Li atoms with Sn, the expected electronic instability can be compensated for because the Fermi level is raised to the proximity of the local DOS minimum. Careful inspection of the DOS plot shows that, within the rigid-band approximation, the calculated E_F (for 29 valence electrons per formula unit) is 0.16 eV below an area of relatively lower DOS, corresponding to 29.4 valence electrons per formula. More importantly, the local minimum at ca. 0.51 eV above E_F is found to correspond to 30.4 valence electrons per formula.

The above-mentioned points regarding the electronic structure of $La_3Li_4Ge_4$ can be reconciled with the Zintl−Klemm formulation; because the structure has two Ge atoms, one isolated and one forming the Ge_2 dimers, the latter should bear a formal charge of "6−" (total). Assigning the rare-earth metal and the Li atoms as electron donors, as was done before for $La_2Li_2Ge_3$, yields $(La^{3+})_3(Li^+)_4(Ge^{4-})_2(Ge^{3-})_2$, which suggests a shortage of a valence electron.

Magnetism. Temperature-dependent dc magnetization measurements were performed on polycrystalline samples of $RE_2Li_2Ge_3$ and $RE_3Li_4Ge_4$ (*RE* = Ce, Pr, Nd, Sm) within the range from 5 to 300 K under an applied field of 5000 Oe. $La_2Li_2Ge_3$ and $La_3Li_4Ge_4$ were not measured because the La^{3+} ion is a closed-shell species and has no unpaired electrons. The data were converted to molar magnetic susceptibility ($\chi_m = M/H$), and the $\chi_m(T)$ plots are shown in Figures 7 and 8. In the high-temperature regime, all samples are paramagnetic as expected for systems with core 4f electrons. The data for $RE_2Li_2Ge_3$ and $RE_3Li_4Ge_4$ (*RE* = Ce, Pr, Nd) compounds follow the Curie−Weiss law $\chi(T) = C/(T - \theta_p)$,[41] *C* is the Curie constant ($N_A\mu_{eff}^2/3k_bT$), and θ_p is the paramagnetic Weiss temperature. Curie constants and effective magnetic moments of $RE_2Li_2Ge_3$ and $RE_3Li_4Ge_4$ (RE = Ce, Pr, Nd) can be calculated from linear fits of the inverse magnetic susceptibility versus temperature and are summarized in Table 7. The moments in all cases are consistent

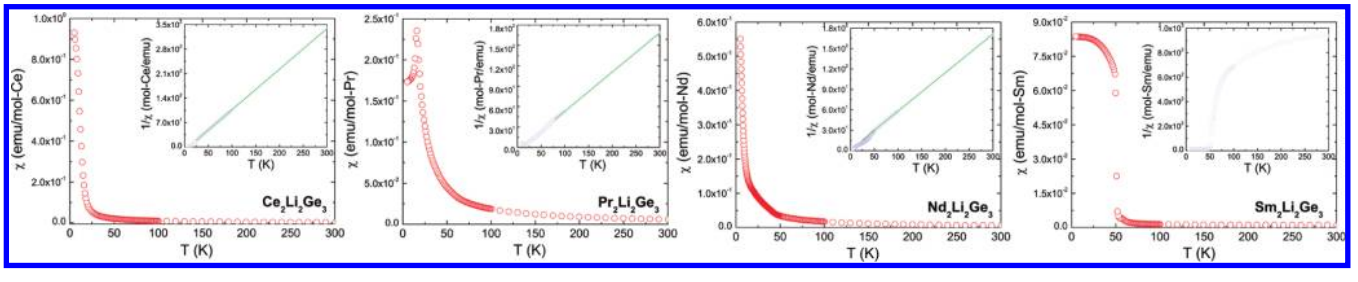

Figure 7. Temperature dependence of the magnetic susceptibility of $RE_2Li_2Ge_3$ (RE = Ce−Nd, Sm). Inset: Inverse susceptibility vs temperature with linear fits to the Curie−Weiss law.

dx.doi.org/10.1021/ic202591j | Inorg. Chem. 2012, 51, 3119−3129

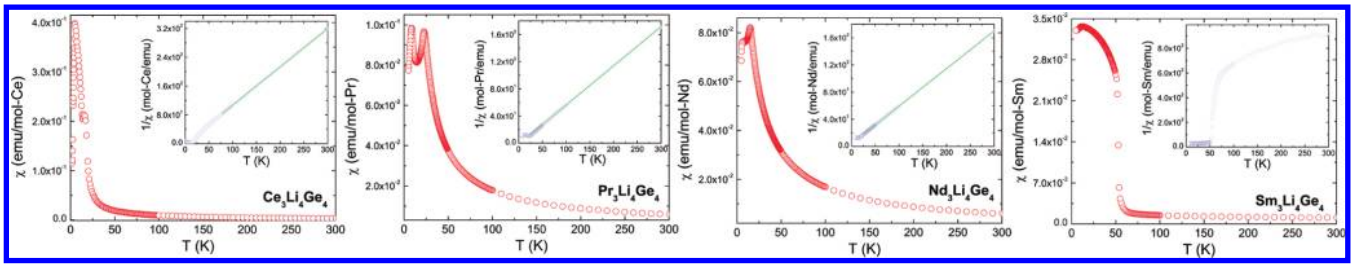

Figure 8. Temperature dependence of the magnetic susceptibility of $RE_3Li_4Ge_4$ (RE = Ce−Nd, Sm). Inset: Inverse susceptibility vs temperature with linear fits to the Curie−Weiss law.

Table 7. Effective Magnetic Moments and Ordering Temperatures of $RE_2Li_2Ge_3$ and $RE_3Li_4Ge_4$ (RE = Ce, Pr, Nd), Determined from Linear Fits to the Inverse Magnetic Susceptibilities

	$Ce_2Li_2Ge_3$	$Pr_2Li_2Ge_3$	$Nd_2Li_2Ge_3$	$Ce_3Li_4Ge_4$	$Pr_3Li_4Ge_4$	$Nd_3Li_4Ge_4$
magnetic order	FM[a]	AFM[a]	FM[a]	FM[a]	AFM[a]	AFM[a]
μ_{eff}/μ_B	2.63	3.72	3.76	2.77	3.71	3.80
μ_{calcd}/μ_B	2.54	3.58	3.62	2.54	3.58	3.62
θ_p/ K	8.5	7.9	−2.7	−0.2	3.0	−7.5
T_N/K		16		15	8.4/22.5	6.3/14.8
T_C/K	11		4	5		

[a]FM and AFM denote ferro- and antiferromagnetic interactions, respectively.

with the magnetic behavior expected for free-ion RE^{3+} according to the Hund's rule.[41] $Sm_2Li_2Ge_3$ and $Sm_3Li_4Ge_4$ show the characteristic Van Vleck-type paramagnetism, where the significant contribution of the temperature-independent term χ_o to the total molar susceptibility is accounted for with the modified Curie−Weiss law $\chi_m(T) = \chi_0 + C/(T - \theta_p)$.[41]

In the low-temperature regime, the magnetization curves for most of the measured samples, excluding $Ce_2Li_2Ge_3$ and $Nd_2Li_2Ge_3$, indicate magnetic ordering phase transitions. For $Ce_2Li_2Ge_3$, down to the lowest attainable temperature (5 K), no apparent signature of magnetic ordering can be detected. However, considering the positive θ_p (8 K) and the inflection point in $\chi_m(T)$ at around 10 K, ferromagnetic interactions between the Ce ions can be inferred. Indeed, as seen from the plot, the magnetization begins to increase sharply at low temperatures (below ca. 20−25 K) and perhaps reaches a plateau just below 5 K. In order to verify this hypothesis, FC and ZFC data were taken; magnetization (M) versus applied field (H) behavior was investigated as well (Supporting Information). The difference between the FC and ZFC data confirms the ferromagnetic correlations; the $M-H$ curve (Supporting Information) at 2 K shows a tendency to magnetically saturate with a saturation moment corresponding to one unpaired electron. An apparent ambiguity also exists for $Nd_2Li_2Ge_3$: the $\chi_m(T)$ curve from the FC data suggests a lack of long-range magnetic order, although the clear difference between the FC and ZFC magnetic susceptibilities indicates the Nd unpaired electrons order ferromagnetically at around 4 K. In order to understand the magnetic response of $Nd_2Li_2Ge_3$, the sample has to be reinvestigated at even lower temperature.

A cusplike feature is visible in the $\chi_m(T)$ data at 16 K for $Pr_2Li_2Ge_3$, indicating the onset of long-range antiferromagnetic ordering in $Pr_2Li_2Ge_3$. The very small positive θ_p seemingly contradicts this conclusion but can be explained assuming the presence of very weak ferromagnetic correlations between the Pr^{3+} ions, which are suppressed by the stronger antiferromagnetic interactions. The last compound of the $RE_2Li_2Ge_3$ (RE = Ce−Nd, Sm) series, $Sm_2Li_2Ge_3$, shows typical ferromagnetic behavior. It can be seen from Figure 7 that the magnetic response for $Sm_2Li_2Ge_3$ reaches saturation below ca. 51 K under a field of 5000 Oe. At 300 K, the effective magnetic moment of the Sm^{3+} ion was calculated to be 1.6 μ_B according to the formula $[8(\chi_m T)]^{1/2}$, which is very close to the effective moment of 1.55 μ_B, calculated by the Van Vleck method.[42]

The molar magnetic susceptibilities of $RE_3Li_4Ge_4$ (RE = Ce−Nd, Sm) as a function of the temperature are plotted in Figure 8. Different from their "2−2−3" counterparts, $Ce_3Li_4Ge_4$, $Pr_3Li_4Ge_4$, and $Nd_3Li_4Ge_4$ all undergo two magnetic transitions, while $Sm_3Li_4Ge_4$ shows magnetic behavior similar to that of $Sm_2Li_2Ge_3$. For $Ce_3Li_4Ge_4$, the FC $\chi_m(T)$ curve shows a magnetic ordering occurring at 15 K, while the diverging FC and ZFC data confirm the second transition at about 5 K. Both ordering transitions are indicative of ferromagnetic correlations. Both $Pr_3Li_4Ge_4$ and $Nd_3Li_4Ge_4$ show two different long-range magnetic ordering temperatures: at 8.4 and 22.5 K and at 6.3 and 14.8 K, respectively. Because there are two crystallographically inequivalent RE sites, 4*j* and 2*a*, respectively (Table 4), it can be concluded that the two ordering temperatures arise from interactions on two different magnetic sublattices. Indeed, previous studies on some isostructural compounds with Cu and Ag, instead of Li, such as $Dy_3Ag_4Sn_4$,[43] $Er_3Cu_4Sn_4$,[44] $Er_3Cu_4Ge_4$,[45] $Tb_3Ag_4Sn_4$,[46] and $Sm_3Ag_4Sn_4$,[47] have reported similar behavior and have proposed that the RE atoms on the 2*a* site order first, i.e., at higher temperature, followed by a second ordering of the RE atoms on the 4*j* site.[43,45] To fully understand the nature of such a complex magnetic response by these three compounds, more investigations by alternating-current magnetometry and neutron diffraction are needed.

CONCLUSIONS

The crystal structures of $RE_2Li_2Ge_3$ and $RE_3Li_4Ge_4$ (RE = La−Nd, Sm) are closely related and contain $REGe_2$ fragments with the AlB_2 structure and $RELi_2Ge$ fragments with the $MgAl_2Cu$ structure. $RE_2Li_2Ge_3$ and $RE_3Li_4Ge_4$ can also be viewed as the first two members of a potentially large $[REGe_2]_n[RELi_2Ge]_m$ homologous series. TB-LMTO-ASA calculation results indicate that, with 20 valence electrons per formula, the $RE_2Li_2Ge_3$ phases have optimized bonding and are energetically stable,

dx.doi.org/10.1021/ic202591j | Inorg. Chem. 2012, 51, 3119−3129

while the structure of the $RE_3Li_4Ge_4$ phases with 29 valence electrons per formula is electron-deficient. The latter compounds exhibit mixing of Li and Ge; i.e., they are $RE_3Li_{4-x}Ge_{4+x}$ ($x \approx 0.1$), which alleviates the apparent shortage of valence electrons. $RE_2Li_2Ge_3$ (*RE* = Ce, Nd, Sm) and $RE_3Li_4Ge_4$ (*RE* = Ce, Sm) order ferromagnetically at cryogenic temperatures, while $Pr_2Li_2Ge_3$ orders antiferromagnetically. $RE_3Li_4Ge_4$ (*RE* = Ce, Pr, Nd) shows two different magnetic transition temperatures. Currently, our efforts are focused on the synthesis and characterization of the higher homologues $RE_7Li_8Ge_{10}$ ($[REGe_2]_3[RELi_2Ge]_4$). We are also pursuing an extension of this chemistry to Sn because preliminary data for $Ce_3Li_{3.69}Sn_{4.31(1)}$ provided important clues on the off-stoichiometry in this structure.

■ ASSOCIATED CONTENT

Supporting Information

A combined X-ray crystallographic file in CIF format, tables with crystallographic information for structure refinements with Li/Ge disorder in $RE_3Li_{4-x}Ge_{4+x}$ ($x \approx 0.1$), tables with crystallographic information for $Ce_3Li_{3.69}Sn_{4.31(1)}$, figure of a representative powder X-ray diffraction pattern matched with the calculated one, figure comparing the structures of $ThCr_2Si_2$ and $MgAl_2Cu$, COHP curves for La1−Ge1, La2−Ge1, La1−Ge2, and La2−Ge2 interactions in $La_3Li_4Ge_4$, ZFC−FC magnetic susceptibility data of $Ce_2Li_2Ge_3$, $Nd_2Li_2Ge_3$, and $Ce_3Li_4Ge_4$, and a *M*−*H* curve for $Ce_2Li_2Ge_3$. This material is available free of charge via the Internet at http://pubs.acs.org.

■ AUTHOR INFORMATION

Corresponding Author

*E-mail: bobev@udel.edu. Phone: (302) 831-8720. Fax: (302) 831-6335.

Present Address

[†]Department of Chemistry, Chungbuk National University, Cheongju, Chungbuk 361-763, South Korea.

Notes

The authors declare no competing financial interest.

■ ACKNOWLEDGMENTS

S.B. acknowledges financial support from the National Science Foundation through Grant DMR-0743916 (CAREER). Work at CBNU was supported by a research grant from the Chungbuk National University in 2011. We thank Nian-Tzu Suen for helpful discussions.

■ REFERENCES

(1) (a) Mudring, A.-V.; Corbett, J. D. *J. Am. Chem. Soc.* **2004**, *126*, 5277−5281. (b) Bobev, S.; Sevov, S. C. *J. Am. Chem. Soc.* **2002**, *124*, 3359−3365. (c) Ganguli, A. K.; Corbett, J. D.; Köckerling, M. *J. Am. Chem. Soc.* **1998**, *120*, 1223−1229. (d) Xu, Z. H.; Guloy, A. M. *J. Am. Chem. Soc.* **1998**, *120*, 7349−7350. (e) Misra, S.; Miller, G. J. *J. Am. Chem. Soc.* **2008**, *130*, 13900−13911. (f) Ponou, S.; Kim, S.-J.; Fässler, T. F. *J. Am. Chem. Soc.* **2009**, *131*, 10246−10252. (g) Tobash, P. H.; Bobev, S. *J. Am. Chem. Soc.* **2006**, *128*, 3532−3533.

(2) Tobash, P. H.; Bobev, S. *J. Solid State Chem.* **2007**, *180*, 1575−1581.

(3) Tobash, P. H.; Bobev, S.; Thompson, J. D.; Sarrao, J. L. *J. Alloys Compd.* **2009**, *488*, 533−537.

(4) (a) Tobash, P. H.; Meyers, J. J.; DiFilippo, G.; Bobev, S.; Ronning, F.; Thompson, J. D.; Sarrao, J. L. *Chem. Mater.* **2008**, *20*, 2151−2159. (b) Tobash, P. H.; Bobev, S.; Ronning, F.; Thompson, J. D.; Sarrao, J. L. *J. Alloys Compd.* **2009**, *488*, 511−517.

(5) Hereafter, *RE* denotes rare-earth metal.

(6) Suen, N.-T.; Tobash, P. H.; Bobev, S. *J. Solid State Chem.* **2011**, *184*, 2941−2947.

(7) Tobash, P. H.; Lins, D.; Bobev, S. *Chem. Mater.* **2005**, *17*, 5567−5573.

(8) Tobash, P. H.; Bobev, S.; Thompson, J. D.; Sarrao, J. L. *Inorg. Chem.* **2007**, *48*, 6641−6651.

(9) You, T.-S.; Tobash, P. H.; Bobev, S. *Inorg. Chem.* **2010**, *49*, 1773−1783.

(10) Bobev, S.; You, T.-S.; Suen, N.-T.; Saha, S.; Greene, R.; Paglione, J.-P. *Inorg. Chem.* **2011**, DOI: 10.1021/ic2021484.

(11) You, T.-S.; Bobev, S. *J. Solid State Chem.* **2010**, *183*, 1258−1265.

(12) Pauling, L. *The Nature of the Chemical Bond*; Cornell University Press: Ithaca, NY, 1960.

(13) Nesper, R. *Prog. Solid State Chem.* **1991**, *1*, 1−45.

(14) You, T.-S.; Bobev, S. *J. Solid State Chem.* **2010**, *183*, 2895−2902.

(15) Grund, I.; Zwiener, G.; Schuster, H.-U. *Z. Anorg. Allg. Chem.* **1986**, *535*, 7−12.

(16) *Handbook of Chemistry and Physics*, 83rd ed.; CRC Press LLC: Boca Raton, FL, 2002.

(17) For both 2:4:3 and 3:8:4 reactions, the unreacted Li was washed using isopropyl alcohol and water.

(18) Merlo, F.; Palenzona, A.; Pani, M.; Dhar, S. K.; Kulkarni, R. *J. Alloys Compd.* **2005**, *394*, 101−106.

(19) (a) *SMART NT*, version 5.63; Bruker Analytical X-ray Systems, Inc.: Madison, WI, 2003. (b) *SAINT NT*, version 6.45; Bruker Analytical X-ray Systems, Inc.: Madison, WI, 2003.

(20) *SADABS NT*, version 2.10; Bruker Analytical X-ray Systems, Inc.: Madison, WI, 2001.

(21) *SHELXTL*, version 6.12; Bruker Analytical X-ray Systems, Inc.: Madison, WI, 2001.

(22) Stoichiometric $A_2Li_2Ge_3$ (*A* = Sr, Ba, Eu) would be electron-deficient and could not be synthesized. Only $A_2(Li_{1-x}In_x)_2Ge_3$ ($x \approx 0.3$), where the valence electron count is augmented by virtue of Li−In substitution, can be obtained.

(23) Gelato, L. M.; Parthé, E. *J. Appl. Crystallogr.* **1987**, *20*, 139−146.

(24) Jepsen, O.; Burkhardt, A.; Andersen, O. K. *The TB-LMTO-ASA Program*, version 4.7; Max-Planck-Institut für Festkörperforschung: Stuttgart, Germany, 1999.

(25) Andersen, O. A.; Jepsen, O.; Glötzel, D. In *Highlights of Condensed Matter Theory*; Bassani, F., Fumi, F., Tosi, M., Eds.; North-Holland: New York, 1985.

(26) Jepsen, O.; Anderson, O. K. *Z. Phys. B* **1995**, *97*, 35−47.

(27) Anderson, O. K.; Jepsen, O. *Phys. Rev. Lett.* **1984**, *53*, 2571−2574.

(28) Lambrecht, W. R. L.; Andersen, O. K. *Phys. Rev. B* **1986**, *34*, 2439−2449.

(29) Dronskowski, R.; Blöchl, P. *J. Phys. Chem.* **1993**, *97*, 8617−8624.

(30) *Pearson's Handbook of Crystallographic Data for Intermetallic Phases*, 2nd ed.; Villars, P., Calvert, L. D., Eds.; American Society for Metals: Materials Park, OH, 1991.

(31) Pavlyuk, V. V.; Pecharskii, V. K.; Bodak, O. I.; Bruskov, V. A. *Kristallografiya* **1988**, *33*, 46−50.

(32) Xie, Q.-X.; Nesper, R. *Z. Kristallogr. - New Cryst. Struct.* **2004**, *219*, 83−84.

(33) Todorov, I.; Sevov, S. C. *Inorg. Chem.* **2005**, *44*, 5361−5369.

(34) Xie, Q.-X.; Nesper, R. *Z. Kristallogr. - New Cryst. Struct.* **2003**, *218*, 289−290.

(35) Liebrich, O.; Schaefer, H.; Weiss, A. *Z. Naturforsch. B* **1970**, *25*, 650−651.

(36) Monconduit, L.; Belin, C. *Acta Crystallogr., Sect. C* **1999**, *55*, 1199−1200.

(37) (a) Kotur, B. Ya.; Sikirica, M. *Acta Crystallogr., Sect. B* **1982**, *38*, 917−918. (b) Weitzer, F.; Hiebl, K.; Rogl, P.; Noël, H. *Ber. Bunsenges. Phys. Chem.* **1992**, *96*, 1715−1717. (c) Rieger, W. *Monatsh. Chem.* **1970**, *101*, 449−462. (d) Pechev, S.; Chevalier, B.; Darriet, B.; Gravereau, P.; Etourneau, J. *J. Alloys Compd.* **1996**, *243*, 77−81.

(38) Strictly speaking, Ge_2 dimers within the two conjoined trigonal prisms of *RE* atoms constitute only a half of the hypothetical $REGe_2$

with the AlB_2 structure type. Thus, the description of the structure of the $RE_3Li_4Ge_4$ compounds as a $^1/_2$:1 intergrowth of the imaginary $REGe_2$ and $RELi_2Ge$ phases will be more appropriate.
(39) Guo, S.-P.; Bobev, S. Unpublished results. $Ce_7Li_8Ge_{10}$ crystallizes in the orthorhombic space group *Cmmm*; $Z = 2$; $a = 6.9158(11)$ Å, $b = 33.667(5)$ Å, $c = 4.4639(7)$ Å, $V = 1039.4(3)$ Å^3; R1 = 0.0310, wR2 = 0.0706, $T = 200$ K.
(40) (a) Guloy, A. M. Polar Intermetallics and Zintl Phases along the Zintl Border. *Inorganic Chemistry in Focus III*; Wiley-VCH Verlag GmbH & Co. KGaA: Weinheim, Germany, 2006. (b) *Chemistry, Structure and Bonding of Zintl Phases and Ions*; Kauzlarich, S. M., Ed.; VCH: Weinheim, Germany, 1996; and references cited therein.
(41) (a) Smart, J. S. *Effective Field Theories of Magnetism*; Saunders: Philadelphia, PA, 1966. (b) Kittel, C. *Introduction to Solid State Physics*, 7th ed.; John Wiley and Sons: Hoboken, NJ, 1996.
(42) Van Vleck, J. H. *The Theory of Electric and Magnetic Susceptibilities*; Oxford University Press: London, 1965.
(43) Perry, L. K.; Cadogan, J. M.; Ryan, D. H.; Canepa, F.; Napoletano, M.; Mazzone, D.; Riani, P. *J. Phys.: Condens. Matter* **2006**, *18*, 5783–5792.
(44) Wawrzynska, E.; Hernandez-Velasco, J.; Penc, B.; Sikora, W.; Szytula, A.; Zygmunt, A. *J. Phys.: Condens. Matter* **2003**, *15*, 5279–5296.
(45) Wawrzynska, E.; Hernandez-Velasco, J.; Penc, B.; Szytula, A.; Zygmunt, A. *J. Magn. Magn. Mater.* **2003**, *264*, 192–201.
(46) Perry, L. K.; Ryan, D. H.; Canepa, F.; Napoletano, M.; Mazzone, D.; Riani, P. *J. Appl. Phys.* **2006**, *99*, 08J502.
(47) Voyer, C. J.; Ryan, D. H.; Cadogan, J. M.; Cranswick, L. M. D.; Napoletano, M.; Riani, P.; Canepa, F. *J. Phys.: Condens. Matter* **2007**, *19*, 436205.